

MiR-101/EZH2 negative feedback signaling drives oxygen–glucose deprivation/reperfusion-induced injury by activating the MAPK14 signaling pathway in SH-SY5Y cells

Hao Gu^{1#}, Qing Chen^{1#} and Jian Li^{2✉}

¹Department of Pediatrics, The Affiliated Huaian No.1 People's Hospital of Nanjing Medical University, Huai'an City, Jiangsu Province, 223300, China; ²Department of Anesthesiology, The Affiliated Huaian No.1 People's Hospital of Nanjing Medical University, Huai'an City, Jiangsu Province, 223300, China

MiR-101 has been reported to be involved in neuroinflammation, neuronal injury and neurotoxicity. However, the specific role and mechanism of miR-101 in ischemia/reperfusion (I/R)-induced neuronal injury remain largely unknown. Our study found that after oxygen–glucose deprivation/reperfusion (OGD/R) exposure, the level of miR-101 in SH-SY5Y cells was significantly decreased, which was accompanied by a decrease in cell viability, and an increase in LDH release and apoptosis. MiR-101 overexpression (miR-101 mimics) significantly promoted viability and inhibited LDH release and apoptosis in OGD/R-exposed SH-SY5Y cells. Luciferase reporter assay indicated that enhancer of zeste 2 polycomb repressive complex 2 subunit (EZH2) was a direct target of miR-101, and EZH2 siRNA obviously increased the viability, inhibited LDH release and apoptosis in OGD/R-exposed SH-SY5Y cells. Besides, EZH2 siRNA could inhibit the activation of mitogen-activated protein kinase (MAPK14) signaling pathway and the MAPK14 agonist (anisomycin) could reverse EZH2 siRNA-induced increase in cell viability, and decreases in LDH release and apoptosis. Furthermore, when the methyltransferase activity of EZH2 was inhibited by its specific inhibitor GSK126, the level of miR-101 was increased in OGD/R-exposed SH-SY5Y cells. Additionally, EZH2 siRNA upregulated miR-101 expression in OGD/R-exposed SH-SY5Y cells. Taken together, our findings reveal that miR-101/EZH2 negative feedback signaling drives OGD/R-induced injury by activating the MAPK14 signaling pathway in SH-SY5Y cells.

Keywords: EZH2, miRNA-101, neuronal injury, ischemia/reperfusion

Received: 23 September, 2021; **revised:** 07 December, 2021; **accepted:** 31 December, 2021; **available on-line:** 26 May, 2022

✉ e-mail: hayyljian@njmu.edu.cn

[#]These authors contributed equally to the manuscript

Acknowledgements of financial support: This work was supported by grants from the Huaian Health Science Program (HAWJ202008), Nanjing Medical University Science and Technology Development Fund under Grant (NMUB2020145), and Young Scientific and Technological Talents Project of Huaian No.1 People's Hospital (QNRC202105).

Abbreviations: HIBD, hypoxic-schemic brain damage; I/R, ischemia/Reperfusion; OGD/R, oxygen–glucose deprivation/reperfusion; PD, parkinson's disease; EZH2, enhancer of zeste homolog 2 methyltransferase; PRC2, polycomb repressive complex 2; H3K27, methylating lysine 27 of histone H3; CNS, central nervous system.

INTRODUCTION

Neuronal injury is considered to play a deleterious role in brain-related diseases, such as stroke, Alzheimer's

disease and neonatal hypoxic-ischemic brain damage (HIBD) (Koehn *et al.*, 2020; Merlo *et al.*, 2019; Sekerdag *et al.*, 2018). Ischemia/reperfusion (I/R) has been demonstrated to be the major cause of neuronal injury (Carbone *et al.*, 2019; Lv *et al.*, 2020; Peng *et al.*, 2019). Thus, the understanding of the molecular mechanism of I/R-evoked neuronal injury will be conducive to developing strategies for improving neuronal survival after I/R-evoked injury.

MicroRNAs have been shown to play a primary role in I/R-evoked neuronal injury (Chen *et al.*, 2020; Ge *et al.*, 2019; Wang *et al.*, 2020b; Yang *et al.*, 2021; Yi *et al.*, 2020; Zhang *et al.*, 2019). Recently, miR-101 was shown to promote Parkinson's disease (PD) by promoting α -synuclein-induced dopaminergic neuron injury (Bu *et al.*, 2020). MiR-101 was also found to be involved in neuroinflammation and neuronal injury in the spinal cord after brachial plexus injury (Liu *et al.*, 2020a). Zhao *et al.* reported that miR-101 plays a vital role in bupivacaine-induced neurotoxicity (Zhao and Ai, 2019). In addition, miR-101 overexpression was demonstrated to alleviate I/R-induced injury in different tissues, such as liver tissue, testicular tissue and renal tissue (Qin *et al.*, 2019; Song *et al.*, 2019a; Zhao *et al.*, 2020). To date, the potential function and mechanism of miR-101 in I/R-evoked neuronal injury remain largely unknown.

Enhancer of zeste 2 polycomb repressive complex 2 subunits (EZH2) can induce transcriptional silencing by methylating lysine 27 of histone H3 (H3K27) (Wang and Wang, 2020). EZH2 plays a significant role in mammalian central nervous system (CNS) development (Chen *et al.*, 2019; Wang *et al.*, 2020c). Recent *in vivo* studies showed that silencing EZH2 ameliorated I/R-induced neuronal injury (Jin *et al.*, 2021; Xue *et al.*, 2019). Furthermore, EZH2 was demonstrated to be a direct target of miR-101 in various cells, such as cancer cells and endothelial cells (Jiang *et al.*, 2019; Liu *et al.*, 2017; Smits *et al.*, 2011). However, whether EZH2 acts as direct target of miR-101 in I/R-evoked neuronal injury remains unknown. In the current study, we investigated the role of miR-101 in I/R-evoked neuronal injury and whether its role depends on EZH2 as well as the potential mechanism involved.

MATERIALS AND METHODS

Experimental reagents

The antibodies against BAX, BAD, BCL2, EZH2, H3K27me3, phospho-NF-KB1, NF-KB1, phospho-

MAPK14, MAPK14, and β -actin were purchased from Cell Signaling Technology (Shanghai, China). Fetal bovine serum (FBS) and cell culture reagents were purchased from Thermo Fisher Scientific, Inc. (Carlsbad, CA). Lipofectamine 2000 was provided by Invitrogen (Shanghai, China). CCK-8 was purchased from Chemicon (Temecula, CA, USA). All the sequences, primers, siRNAs were designed and provided by Shanghai Genechem Co. (Shanghai, China).

Cell culture

SH-SY5Y cells were obtained from Zhong Qiao Xin Zhou Biotechnology Co., Ltd (Cat. No.ZQ0050, Shanghai, China) and cultured in MEM/F12 medium (Zhong Qiao Xin Zhou Biotechnology Co., Ltd.) supplemented with 10% fetal bovine serum (FBS, Thermo Fisher Scientific, Inc.), 1% sodium pyruvate, 2 mmol/L L-glutamine, 1% L-alanyl-L-glutamine, 100 μ g/mL streptomycin and 100 U/mL penicillin at 37°C in a humidified atmosphere with 5% CO₂. Cells were passaged every 3–4 days until they reached 80%–90% confluence, and the logarithmic growth phase cells were prepared for subsequent experiment. Cells were subjected to mycoplasma and microbial contamination examination every 3–4 months in our laboratory. Cells were plated in 96-well culture plates at a density of 1×10⁴ cells/well for the cytotoxicity assays, or 60-mm culture dishes at a density of 1×10⁶ cells/well for qPCR, flow cytometry, and western blot. For neuronal differentiation, SH-SY5Y cells were cultured for 5 days with 10 μ M retinoic acid (RA) in MEM/F12 plus 10% FBS, 2 mmol/L glutamine, and antibiotics, followed by another 5 days culture in serum-free MEM/F12 with brain-derived neurotrophic factor (BDNF, 50 ng/mL) and glutamine (2 mmol/L) and antibiotics.

OGD/R induction

For OGD/R induction, SH-SY5Y cells were cultured in glucose-free MEM/F12 medium without serum and then transferred to the AnaeroPack™ container containing a gas mixture of 0% O₂, 95% N₂ and 5% CO₂ for 4 h at 37°C. The oxygen content in the container was checked using a disposable anaerobic indicator strip. The cells were then cultured in normal MEM/F12 medium for 24 h under normoxic conditions. SH-SY5Y cells cultured in normal MEM/F12 medium under normoxic conditions served as a control.

Cell transfection

The EZH2 siRNA, control siRNA, miR-101 mimic, and control mimic were obtained from GenePharm (Shanghai, China). SH-SY5Y cells were transfected with these oligonucleotides by using Lipofectamine 2000 reagent (Invitrogen, Carlsbad, CA, USA) following the protocol of the manufacturer. Briefly, transfection was performed in 6-well plates when the cells' confluence was about 80%–90%. A mixture of siRNAs or mimics and Lipofectamine 2000 was slowly added into the wells. After transfection, the cells were cultured for 48 h and applied for the further experiment assay, or for the verification of EZH2 siRNA silencing and miR-101 mimic transfection by western blotting and RT-qPCR, respectively. Control mimic and miR-101 mimic sequences were as follows: control-mimic, 5'-UUCUCCGAACGU GUCACGUTT-3'; miR-101 mimic, 5'-UACAGUACU GUGAUAACUGAA-3'. Control siRNA and miR-101 siRNA sequences were as follows: control siRNA,

5'-UUCUCCGAACGUGUCACGU-3'; EZH2 siRNA, 5'-CCAUGUUUACAACUAUCAA-3'.

Cell viability analysis

A Cell Counting (CCK-8) assay was used to evaluate the viability of SH-SY5Y cells. SH-SY5Y cells were seeded into 96-well plates at a density of 1×10⁴ per well. After treatment as described in the text, CCK-8 solution (20 μ L/well) was added to the cultured cells and incubated for 2 h at 37°C. The absorbance at 450 nm was measured using a plate reader (ELx800, BioTek Instruments, Inc., Vermont, USA). The cell viability of the control group was expressed as a value of 100%, and the cell viability of the other groups was normalized to this value.

Hoechst staining

SH-SY5Y cells were seeded onto coverslips coated with 0.1% gelatin (Sigma, St. Louis, MO) and cultured under normal or OGD/R conditions. Cells were fixed with 4% paraformaldehyde for 30 min, then stained with Hoechst 33258 (5 μ g/mL) for 15 min at room temperature, and then washed to remove unbound dye. The cells were observed and photographed under a fluorescence microscope.

Luciferase reporter assay

The wild type (WT) or mutant (MUT) luciferase reporter vector of the 3'-untranslated region (UTR) of EZH2 containing miR-101 binding sequences was synthesized by Promega (Shanghai, China). Cells were cotransfected with the indicated vectors and the miR-101 mimic or control mimic using Lipofectamine 2000 reagent (Invitrogen). The relative luciferase activity was analyzed using a dual-luciferase reporter assay (Promega) according to the manufacturer's protocol.

Western blotting

After treatment, SH-SY5Y cells were lysed in RIPA lysis buffer (Beyotime). The detailed protocol of Western blotting assay was described previously (Gu *et al.*, 2021). Each lane in the SDS-PAGE gel was loaded with exactly the same amount of quantified protein lysates (30 μ g per sample). The dilution ratios of antibodies were as follows: anti-BAX (1/1000), anti-BAD (1/1000), anti-BCL2 (1/1000), anti-EZH2 (1/2000), anti-H3K27me3 (1/2000), anti-phospho-NFKB1 (1/1000), anti-NFKB1 (1/1000), anti-phospho-MAPK14 (1/1000), anti-MAPK14 (1/1000), and anti- β -actin (1/1000). For data quantification, each band was quantified via the Gel-Pro image program (Media Cybernetics, Las Vegas, USA).

Quantitative reverse transcription PCR (RT-qPCR)

Total RNA was extracted by Trizol reagents (Invitrogen, Shanghai, China) and quantified. miR-101 quantitative PCR was conducted using mirVana™ qRT-PCR miRNA Detection Kit (Ambion, Austin, U.S.A.) in conjunction with a SYBR Green PCR Kit (Thermo Fisher Scientific, MA, U.S.A.) in an ABI PRISM® 7300 real-time PCR system (Applied Biosystems). The PCR amplification parameters were 95°C for 5 min, followed by 40 cycles of 95°C for 15 s, 60°C for 30 s and 72°C for 30 s. After PCR, the 2^{- $\Delta\Delta$ Ct} comparative method was used to calculate the Ct for the relative level of miR-101. The miR-101 level was normalized to that of U6. Gene-specific primers of miR-101 for qRT-PCR analyses were

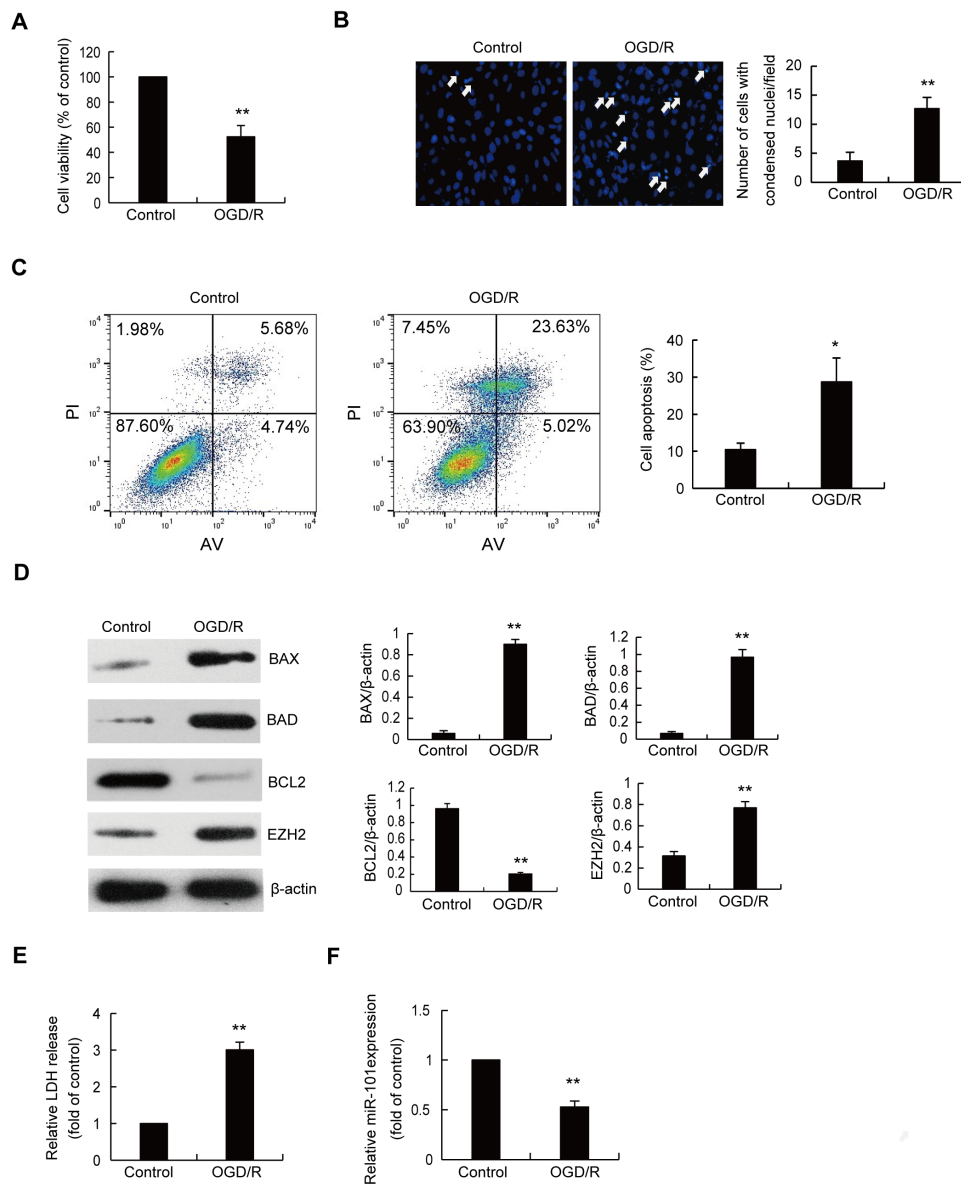


Figure 1. Effects of OGD/R on cell injury, and miR-101 and EZH2 expression in SH-SY5Y cells.

SH-SY5Y cells were subjected to 4 h of oxygen–glucose deprivation followed by reperfusion for 24 h (OGD/R). Control cells were cultured in normal medium under normal condition for the same times. Cell viability was assessed with CCK-8 assays (A). Nuclear morphology changes in SH-SY5Y cells were evaluated with Hoechst 33258 staining, and the number of cells containing condensed chromosomes was calculated (B). Cell apoptosis was examined using flow cytometry with annexinV/PI double staining and the percentages of cells obtained are indicated in each quadrant (C). The expression levels of apoptosis-related proteins and EZH2 were determined by western blot (D). The LDH content in the supernatants of SH-SY5Y cells was measured with a specific kit (E). The expression level of miR-101 was determined by RT-qPCR (F). * $P < 0.05$, ** $P < 0.01$ vs. control group, $n = 3/\text{group}$.

listed as follows: miR-101-F, 5'-GTACAGTACTGT-GATAACTGA-3' and miR-101-R 5'-TGCGTGTCTGTG GAGTC-3'; U6-F, 5'-ATTGGAACGATACAGA-GAAGATTAG-3' and U6-R, 5'-TGCGTGTCTGTG-GAGTC-3'. The relative miR-101 level of the control group was expressed as a value of 1, and the miR-101 levels of the other groups were normalized to this value.

Lactate dehydrogenase (LDH) cytotoxicity assay

The LDH content in the supernatants of SH-SY5Y cells was measured by using an LDH detection kit (Nanjing Jian-cheng Bioengineering Institute, Jiangsu, China). In brief, SH-SY5Y cells were cultured in 96-well plates (1×10^4 per well) for 24 h and then subjected to OGD/R

treatment as described above. After treatment, the LDH released from cells was detected using LDH assay kit according to the manufacturer's instructions. Absorbance was measured at 450 nm, and the LDH released level of the control group was expressed as 1, and the LDH released levels of the other groups were normalized to this value.

Flow cytometry analysis

An AnnexinV-FITC Apoptosis Detection Kit (Beyotime, Nanjing, China) was used to detect cell apoptosis. SH-SY5Y cells were collected and resuspended in binding buffer, followed by double-staining with annexin V-FITC and propidium iodide (PI) dyes ($10 \mu\text{g}/\text{mL}$) for 20

min in the dark at room temperature. The stained cells were analyzed by using a FACSCalibur flow cytometer (BD Biosciences, San Jose, CA) with Cell Quest software (BD Biosciences). The percentages of early apoptotic cells and late apoptotic cells were calculated.

Statistical analysis

The data were presented as mean \pm standard deviation (S.D.), and all trials were repeated three times. The data were analyzed by SPSS software version 15.0 (SPSS Inc., Chicago, IL). Student's *t* test and one-way analysis of variance (ANOVA) along with Tukey's post hoc test were used to gauge the differences between two or multiple groups. $P < 0.05$ was deemed statistically significant.

RESULTS

OGD/R induced cell injury, miR-101 downregulation and EZH2 upregulation in SH-SY5Y cells

As shown in Fig. 1A, the viability of SH-SY5Y cells was decreased significantly after OGD/R treatment.

Hoechst staining showed that OGD/R treatment led to a significant increase in cells containing condensed chromosomes (Fig. 1B). Flow cytometry analysis showed that the percentage of apoptotic cells was remarkably elevated in the OGD/R-treated SH-SY5Y cells compared with the control cells (Fig. 1C). The protein expression levels of proapoptotic BAX and BAD were significantly increased, while the expression of antiapoptotic BCL2 was obviously decreased after OGD/R treatment (Fig. 1D). Moreover, OGD/R treatment led to an increase in LDH release (Fig. 1E). RT-qPCR showed that miR-101 expression was obviously downregulated in OGD/R-exposed SH-SY5Y cells (Fig. 1F). The expression level of EZH2 was significantly upregulated in OGD/R-exposed SH-SY5Y cells (Fig. 1D). The above data suggest that OGD/R evokes cell injury, downregulates miR-101 expression and upregulates EZH2 expression in SH-SY5Y cells.

Upregulation of miR-101 attenuated OGD/R-evoked SH-SY5Y cell injury

To investigate the potential role of miR-101 in OGD/R-evoked cell injury, SH-SY5Y cells were trans-

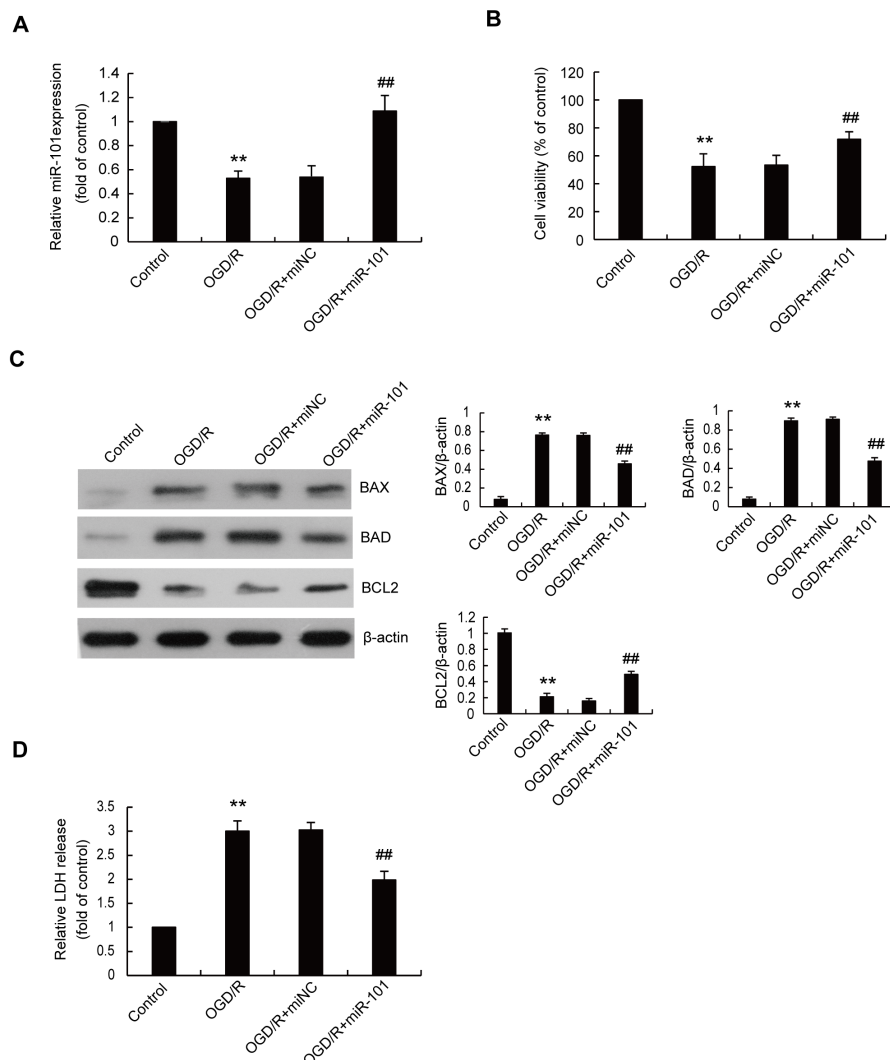


Figure 2. Upregulation of miR-101 attenuated OGD/R-evoked SH-SY5Y cell injury.

SH-SY5Y cells were transfected with the mimic control (miNC) or miR-101 mimic (miR-101) for 24 h, and the cells were then cultured under OGD/R conditions. The expression level of miR-101 was determined by RT-qPCR (A). Cell viability was assessed with CCK-8 assays (B). The expression levels of apoptosis-related proteins were determined by western blot (C). The LDH content was measured with a specific kit (D). ** $P < 0.01$ vs. control group; ## $P < 0.01$ vs. OGD/R + miNC group, $n = 3$ /group.

fectured with the miR-101 mimic, which markedly upregulated miR-101 expression under OGD/R conditions (Fig. 2A). CCK-8 assays showed that miR-101 upregulation significantly increased the viability of OGD/R-exposed SH-SY5Y cells (Fig. 2B). The increased expression levels of BAX and BAD, and the decreased expression level of BCL2 were obviously reversed by miR-101 upregulation in OGD/R-exposed SH-SY5Y cells (Fig. 2C). Furthermore, miR-101 upregulation also significantly inhibited OGD/R-induced LDH release (Fig. 2D). The above data suggest that the upregulation of miR-101 attenuates OGD/R-evoked SH-SY5Y cell injury.

EZH2 acted as a direct target of miR-101 during OGD/R-evoked SH-SY5Y cell injury

To investigate the potential target of miR-101, the expression level of EZH2 was first examined as it was demonstrated to be a direct target of miR-101 in various cell types (Jiang *et al.*, 2019; Liu *et al.*, 2017; Smits

et al., 2011). As shown in Fig. 3A, OGD/R treatment led to a significant increase in EZH2 expression, while miR-101 upregulation obviously downregulated EZH2 expression, indicating that EZH2 is a direct target of miR-101 in OGD/R-exposed SH-SY5Y cells. Based on these findings, a luciferase reporter assay was performed. As shown in Fig. 3B, a significant decrease in luciferase activity was observed in SH-SY5Y cells cotransfected with the miR-101 mimic and the wild-type 3'-UTR of EZH2. However, SH-SY5Y cells cotransfected with the miR-101 mimic and the mutant 3'-UTR of EZH2 showed no obvious difference in luciferase activity. The above data suggest that EZH2 is a direct target of miR-101 in SH-SY5Y cells under OGD/R conditions.

The involvement of EZH2 in OGD/R-evoked SH-SY5Y cell injury was then investigated. As shown in Fig. 3C, OGD/R-induced EZH2 upregulation was markedly inhibited by EZH2 siRNA (Fig. 3C). EZH2 siRNA obviously increased the viability of OGD/R-

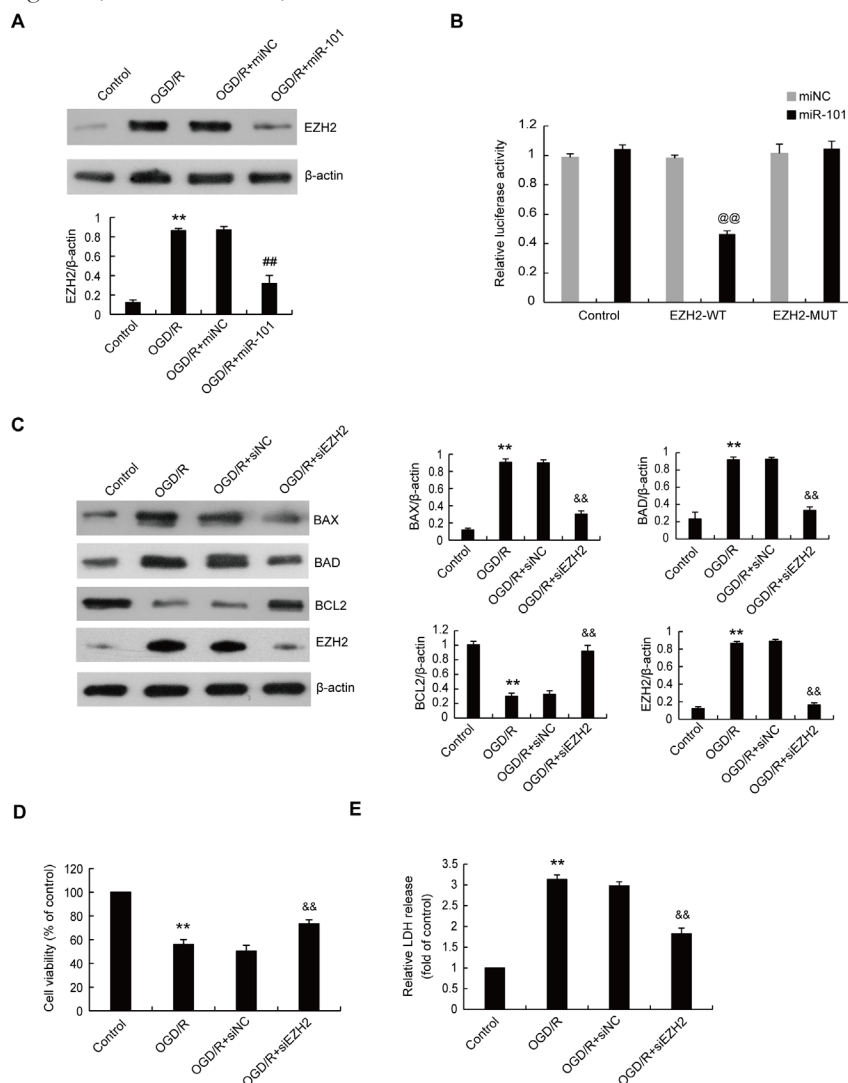


Figure 3. OGD/R downregulated miR-101 to upregulate EZH2 and induced cell injury in SH-SY5Y cells.

(A) SH-SY5Y cells were transfected with the mimic control (miNC) or miR-101 mimic (miR-101) for 24 h, and the cells were then cultured under OGD/R conditions. The expression level of EZH2 was determined by western blot. (B) Luciferase activity was analyzed in cells cotransfected with the wild type (WT) or mutant (MUT) 3'UTR of EZH2 with the control mimic (miNC) or miR-101 mimic (miR-101). (C–E) SH-SY5Y cells were transfected with the negative control siRNA (siNC) or EZH2 specific siRNA (siEZH2) for 24 h, and then cultured under OGD/R conditions. The expression levels of apoptosis-related proteins and EZH2 were determined by western blot (C). Cell viability was assessed with CCK-8 assays (D). The LDH content was measured with a specific kit (E). ** $P < 0.01$ vs. control group; ## $P < 0.01$ vs. OGD/R + miNC group; @@ $P < 0.01$ vs. control + mi101 group; && $P < 0.01$ vs. OGD/R + siNC group; n=3/group.

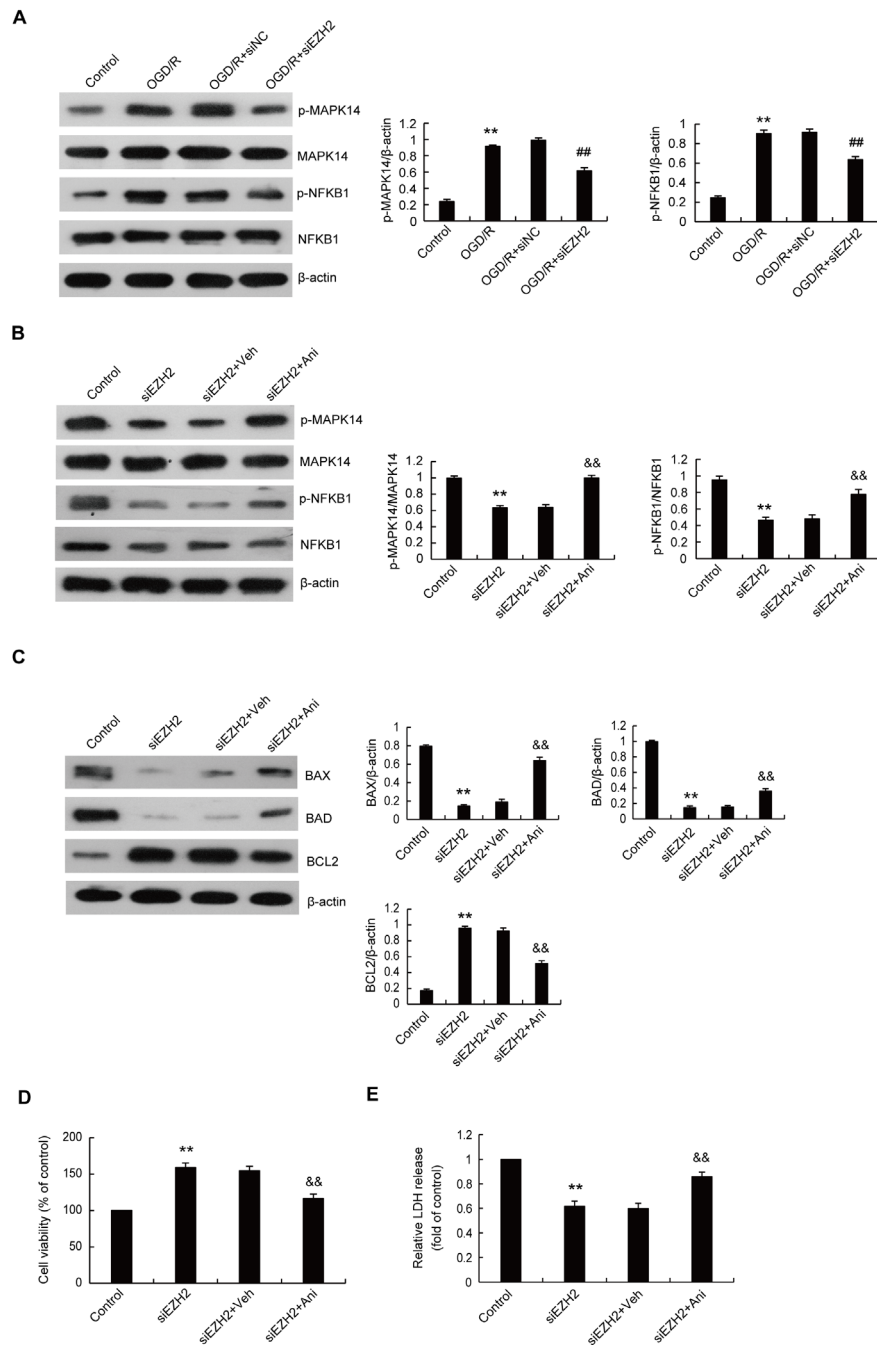


Figure 4. Activation of MAPK14 signaling is required for EZH2-mediated SH-SY5Y cell injury under OGD/R conditions.

(A) SH-SY5Y cells were transfected with the negative control siRNA (siNC) or EZH2 specific siRNA (siEZH2) for 24 h, and the cells were then cultured under OGD/R conditions. The expression and phosphorylation levels of MAPK14 and NFKB1 were measured by western blot. (B–E) siNC or siEZH2-transfected SH-SY5Y cells were treated with vehicle (Veh) or anisomycin (Ani), and cells were then cultured under OGD/R conditions. The expression and phosphorylation levels of MAPK14 and NFKB1 were measured by western blot (B). The expression levels of apoptosis-related proteins were determined by western blot (C). Cell viability was assessed with CCK-8 assays (D). The LDH content was measured with a specific kit (E). ** $P < 0.01$ vs. control group; ## $P < 0.01$ vs. OGD/R + siNC group; && $P < 0.01$ vs. siEZH2 + vehicle group; $n = 3$ /group.

exposed SH-SY5Y cells (Fig. 3D). The increased expression levels of BAX and BAD, and the decreased expression level of BCL2 were significantly reversed by EZH2 siRNA in OGD/R-exposed SH-SY5Y cells (Fig. 3C). Moreover, EZH2 siRNA notably inhibited OGD/R-induced LDH release (Fig. 3E). Taken together, the above data suggest that EZH2 acts as a direct target of miR-101 during OGD/R-evoked SH-SY5Y cell injury.

EZH2 mediated OGD/R-evoked cell injury by activating the MAPK14 signaling pathway

To further investigate the mechanism of EZH2-mediated cell injury under OGD/R conditions, the activation of the MAPK14 signaling pathway was examined. As shown in Fig. 4A, the phosphorylation level of MAPK14 was significantly increased after OGD/R treatment, while the total expression level of MAPK14 remained unchanged. OGD/R treatment also led to an

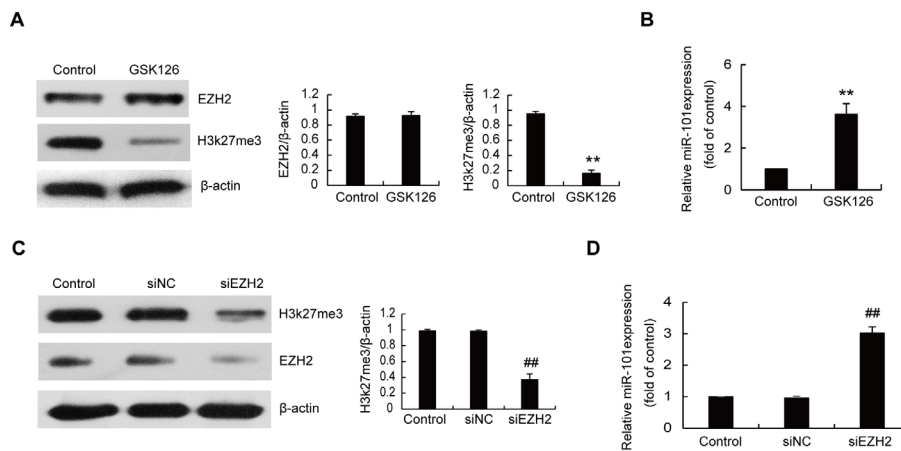


Figure 5. EZH2 regulates miR-101 expression in SH-SY5Y cells under OGD/R conditions.

(A–B) SH-SY5Y cells were treated with or without GSK126, and then cultured under OGD/R conditions. The expression levels of EZH2 and H3K27me3 were measured by western blot (A). The expression level of miR-101 was determined by RT-qPCR (B). (C–D) SH-SY5Y cells were transfected with the negative control siRNA (siNC) or EZH2 specific siRNA (siEZH2) for 24 h, and then cultured under OGD/R conditions. The expression levels of EZH2 and H3K27me3 were measured by western blot (C). The expression level of miR-101 was determined by RT-qPCR (D). ** $P < 0.01$ vs. control group; ## $P < 0.01$ vs. siNC group; $n = 3$ /group.

obvious increase in the phosphorylation level of NFKB1 (Fig. 4A), a well-known downstream target of MAPK14, during I/R-induced injury in various cells, including neuronal cells (Cai *et al.*, 2021; Li *et al.*, 2021; Liu *et al.*, 2020c; Wang *et al.*, 2020a; Xu *et al.*, 2021). EZH2 siRNA significantly reduced the OGD/R-induced phosphorylation of MAPK14 and NFKB1 (Fig. 4A). In OGD/R-exposed SH-SY5Y cells, the EZH2 siRNA-induced inactivation of MAPK14 and NFKB1 was markedly reversed by anisomycin, the MAPK14 agonist (Fig. 4B). Anisomycin treatment significantly reversed EZH2 siRNA-induced BAX and BAD downregulation and BCL2 upregulation in OGD/R-exposed SH-SY5Y cells (Fig. 4C). The EZH2 siRNA-induced increase in cell viability and decreased release of LDH were also significantly inhibited by anisomycin (Fig. 4D–4E). The above data suggest that EZH2 mediates OGD/R-evoked cell injury by activating the MAPK14 signaling pathway.

Reciprocal regulation between miR-101 and EZH2 in OGD/R-exposed SH-SY5Y cells

It has been previously reported that EZH2 regulates miR-101 expression in cancer cells (Wu *et al.*, 2018). To examine whether miR-101 expression in OGD/R-exposed SH-SY5Y cells was also modulated by EZH2 in our system, the methyltransferase activity of EZH2 was inhibited by GSK126. As shown in Fig. 5A, the expression of EZH2 remained unchanged after GSK126 treatment. However, GSK126 treatment significantly downregulated H3K27me3 expression in OGD/R-exposed SH-SY5Y cells. GSK126 also upregulated miR-101 expression (Fig. 5B). Decreased H3K27me3 levels and miR-101 upregulation were observed in OGD/R-exposed SH-SY5Y cells after EZH2 siRNA transfection (Fig. 5C–5D). The above data suggest that miR-101 and EZH2 reciprocally regulate each other during OGD/R-evoked SH-SY5Y cell injury.

DISCUSSION

Accumulating evidence has demonstrated the important role of miR-101 in neuroinflammation, neuronal injury and neurotoxicity (Bu *et al.*, 2020; Liu *et al.*, 2020a;

Zhao and Ai, 2019), but its role in I/R-evoked neuronal injury is not well understood. In the present study, we found that OGD/R induced injury in SH-SY5Y cells, concurrently with the downregulation of miR-101. OGD/R-evoked SH-SY5Y cell injury was significantly diminished when miR-101 expression was upregulated. These results suggest that miR-101 downregulation contributes to I/R-evoked neuronal injury. Based on this finding, the mechanism underlying the promotional effect of miR-101 downregulation on I/R-evoked neuronal injury was investigated.

EZH2, a methyltransferase component of polycomb repressive complex 2 (PRC2), was reported to be the direct target of miR-101 in different types of cells (Jiang *et al.*, 2019; Liu *et al.*, 2017; Smits *et al.*, 2011). Previous studies demonstrated that EZH2 knockdown could attenuate cerebral ischemia-reperfusion injury (Jin *et al.*, 2021; Xue *et al.*, 2019). Therefore, we investigated whether EZH2 served as a direct target of miR-101 in our system. Our results showed that EZH2 expression was increased in OGD/R-exposed SH-SY5Y cells and that miR-101 targeted the 3'UTR of EZH2 to inhibit its expression. Furthermore, silencing EZH2 with a siRNA significantly attenuated OGD/R-evoked SH-SY5Y cell injury. According to the above results, EZH2 acts as a direct target of miR-101 during OGD/R-evoked SH-SY5Y cell injury. As a miRNA, miR-101 was shown to target different downstream proteins under I/R conditions (Kim *et al.*, 2014; Li *et al.*, 2019; Qin *et al.*, 2019; Song *et al.*, 2019a; Zhao *et al.*, 2020). It will be interesting to determine whether other targets of miR-101 associated with neuronal injury and their crosstalk with EZH2 are reproduced in our system.

Further study on the mechanism of miR-101/EZH2-mediated neuronal injury showed that MAPK14 signaling was involved. We focused our investigation on MAPK14 because previous reports showed that the activation of MAPK14 signaling was regulated by EZH2 (Liang *et al.*, 2019; Moore *et al.*, 2013). Moreover, the activation of MAPK14 signaling was shown to exacerbate I/R-induced injury in different tissues, including cerebral tissue (Ali *et al.*, 2021; Liang *et al.*, 2019; Song *et al.*, 2020; Wang *et al.*, 2015). In the present study, EZH2 suppression by an siRNA significantly inhibited the OGD/R-in-

duced activation of MAPK14 and NFKB1, a well-known downstream target of MAPK14, during I/R-induced cell injury (Cai *et al.*, 2021; Li *et al.*, 2021; Liu *et al.*, 2020c; Wang *et al.*, 2020a; Xu *et al.*, 2021). When the activity of MAPK14 was upregulated by anisomycin, the inhibitory effect of EZH2 suppression on OGD/R-evoked SH-SY5Y cell injury was dramatically diminished, indicating that miR-101/EZH2-mediated neuronal injury may be due to an increase in MAPK14 activity. Previous studies reported that the expression and activity of EZH2 were regulated by MAPK14 signaling (Anwar *et al.*, 2018; Nishioka *et al.*, 2015; Ozes *et al.*, 2018). Whether MAPK14 affects EZH2 expression or activity in our system is another interesting point for us to investigate in the near future.

In the investigation of the mechanisms involved in OGD/R-induced miR-101 downregulation in SH-SY5Y cells, we found that EZH2 suppression markedly upregulated miR-101 expression in OGD/R-exposed SH-SY5Y cells, indicating a reciprocal regulation between miR-101 and EZH2 in OGD/R-exposed SH-SY5Y cells. This finding is similar to those of previous reports (i.e., a feedback loop exists between EZH2 and miRNAs in many tumors, such as the EZH2/miR-26 feedback loop in hepatocellular carcinoma, the EZH2/miR-101 feedback loop in multiple myeloma and the EZH2/miR-141 feedback loop in epithelial ovarian cancer) (Deng *et al.*, 2017; Liu *et al.*, 2020b; Song *et al.*, 2019b; Wu *et al.*, 2018; Zhuang *et al.*, 2016). As a methyltransferase component of PRC2, EZH2 was shown to silence the transcription of specific genes and mediate chromatin compaction by catalyzing the trimethylation of histone H3 at lysine 27 (H3K27me3) and directly interacting with DNA methyltransferase, respectively (Li *et al.*, 2020; Liu *et al.*, 2018; Wu *et al.*, 2017). In the present study, when the methyltransferase activity of EZH2 was inhibited by GSK126, OGD/R-induced miR-101 downregulation and H3K27me3 upregulation were obviously reversed. Therefore, we conclude that EZH2 inhibits the expression of miR-101 by catalyzing H3K27me3.

OGD/R of SH-SY5Y cells has been widely used to investigate neuronal injury or death caused by I/R due to the similar properties of SH-SY5Y cells with neurons in morphology, neurochemistry, and electrophysiology (Cai *et al.*, 2021; Jin *et al.*, 2020; Shan *et al.*, 2021). However, use of SH-SY5Y cells as OGD/R cell model involves some limitations. Firstly, SH-SY5Y cells were originated from the parental neuroblastoma cell line SK-N-SH and have undergone clonal changes through three rounds of clonal selection (Kovalevich *et al.*, 2021). Secondly, although differentiated SH-SY5Y cells have a functionally mature neuronal phenotype (Kovalevich *et al.*, 2021; Shipley *et al.*, 2016), whether it has similar expression profiles of proteins or miRNAs with mature neurons in the human brain after OGD/R exposure remains unclear. To overcome the limitation of cell line systems, further studies are needed to confirm our findings with primary neurons.

In conclusion, our study demonstrated that miR-101 and EZH2 form a negative feedback loop and drive OGD/R-induced injury by activating the MAPK14 signaling pathway in SH-SY5Y cells. Although an *in vivo* study is still needed, our findings are of potential pathophysiological importance for understanding the molecular mechanisms of I/R-evoked neuronal injury in brain-related diseases.

Competing interests

The authors declare that they have no competing interests.

Ethical approval

Not applicable.

Statement of Informed Consent

Not applicable.

Availability of data and materials

The datasets used during the present study are available from the corresponding author upon reasonable request.

Authors' contributions

Jian Li supervised the study, Hao Gu wrote the manuscript and analyzed the experimental data, Hao Gu and Qing Chen performed the experiments. All authors read and approved the final manuscript.

REFERENCE

- Ali FEM, Saad Eldien HM, Mostafa NAM, Almaeen AH, Marzouk MRA, Eid KM, Ghaziz AHE, Ebrahiem AF, Hagag MG, Ghogar OM (2021) The impact of royal jelly against hepatic ischemia/reperfusion-induced hepatocyte damage in rats: The role of cytoglobin, Nrf-2/HO-1/COX-4, and P38-MAPK/NF-kappaB-p65/TNF-alpha signaling pathways. *Curr Mol Pharmacol* **14**: 88–100. <https://doi.org/10.2174/1874467213666200514223829>
- Anwar T, Arellano-Garcia C, Ropa J, Chen YC, Kim HS, Yoon E, Grigsby S, Basrur V, Nesvizhskii AI, Muntean A, Gonzalez ME, Kidwell KM, Nikolovska-Coleska Z, Kleer CG (2018) p38-mediated phosphorylation at T367 induces EZH2 cytoplasmic localization to promote breast cancer metastasis. *Nat Commun* **9**: 2801. <https://doi.org/10.1038/s41467-018-05078-8>
- Bu LL, Xie YY, Lin DY, Chen Y, Jing XN, Liang YR, Peng SD, Huang KX, Tao EX (2020) LncRNA-T199678 Mitigates alpha-synuclein-induced dopaminergic neuron injury via miR-101-3p. *Front Aging Neurosci* **12**: 599246. <https://doi.org/10.3389/fnagi.2020.599246>
- Cai SC, Yi CA, Hu XS, Tang GY, Yi LM, Li XP (2021) Isoquercitrin upregulates aldolase C through Nrf2 to ameliorate OGD/R-induced damage in SH-SY5Y cells. *Neurotox Res* **39**: 1959–1969. <https://doi.org/10.1007/s12640-021-00430-1>
- Carbone F, Bonaventura A, Montecucco F (2019) Neutrophil-related oxidants drive heart and brain remodeling after ischemia/reperfusion injury. *Front Physiol* **10**: 1587. <https://doi.org/10.3389/fphys.2019.01587>
- Chen J, Zhang YC, Huang C, Shen H, Sun B, Cheng X, Zhang YJ, Yang YG, Shu Q, Yang Y, Li X (2019) m(6)A Regulates neurogenesis and neuronal development by modulating histone methyltransferase Ezh2. *Genomics Proteomics Bioinformatics* **17**: 154–168. <https://doi.org/10.1016/j.gpb.2018.12.007>
- Chen X, Zhang S, Shi P, Su Y, Zhang D, Li N (2020) MiR-485-5p promotes neuron survival through mediating Rac1/Notch2 signaling pathway after cerebral ischemia/reperfusion. *Curr Neurovasc Res* **17**: 259–266. <https://doi.org/10.2174/1567202617666200415154822>
- Deng M, Zhang R, He Z, Qiu Q, Lu X, Yin J, Liu H, Jia X, He Z (2017) TET-Mediated Sequestration of miR-26 Drives EZH2 expression and gastric carcinogenesis. *Cancer Res* **77**: 6069–6082. <https://doi.org/10.1158/0008-5472.CAN-16-2964>
- Ge XL, Wang JL, Liu X, Zhang J, Liu C, Guo L (2019) Inhibition of miR-19a protects neurons against ischemic stroke through modulating glucose metabolism and neuronal apoptosis. *Cell Mol Biol Lett* **24**: 37. <https://doi.org/10.1186/s11658-019-0160-2>
- Gu H, Li J, Zhang R (2021) Melatonin upregulates DNA-PKcs to suppress apoptosis of human umbilical vein endothelial cells via inhibiting miR-101 under H₂O₂-induced oxidative stress. *Mol Cell Biochem* **476**: 1283–1292. <https://doi.org/10.1007/s11010-020-03991-5>
- Jiang M, Xu B, Li X, Shang Y, Chu Y, Wang W, Chen D, Wu N, Hu S, Zhang S, Li M, Wu K, Yang X, Liang J, Nie Y, Fan D (2019) O-GlcNAcylation promotes colorectal cancer metastasis via the miR-101-O-GlcNAc/EZH2 regulatory feedback circuit. *Oncogene* **38**: 301–316. <https://doi.org/10.1038/s41388-018-0435-5>
- Jin D, Wei W, Song C, Han P, Leng X (2021) Knockdown EZH2 attenuates cerebral ischemia-reperfusion injury via regulating micro-

- RNA-30d-3p methylation and USP22. *Brain Res Bull* **169**: 25–34. <https://doi.org/10.1016/j.brainresbull.2020.12.019>
- Jin W, Xu W, Zhang X, Ren CC (2020) Ischemic preconditioning upregulates decoy receptors to protect SH-SY5Y cells from OGD induced cellular damage by inhibiting TRAIL pathway and agitating PI3K/Akt pathway. *Mol Neurobiol* **57**: 3658–3670. <https://doi.org/10.1089/ars.2014.5856>
- Kim JH, Lee KS, Lee DK, Kim J, Kwak SN, Ha KS, Choe J, Won MH, Cho BR, Jeoung D, Lee H, Kwon YG, Kim YM (2014) Hypoxia-responsive microRNA-101 promotes angiogenesis via heme oxygenase-1/vascular endothelial growth factor axis by targeting cullin 3. *Antioxid Redox Signal* **21**: 2469–2482. <https://doi.org/10.3390/ijms21239193>
- Koehn LM, Chen X, Logsdon AF, Lim YP, Stonestreet BS (2020) Novel neuroprotective agents to treat neonatal hypoxic-ischemic encephalopathy: Inter-alpha inhibitor proteins. *Int J Mol Sci* **21**. <https://doi.org/10.3390/ijms21239193>
- Kovalevich J, Santerre M, Langford D (2021) Considerations for the Use of SH-SY5Y neuroblastoma cells in neurobiology. *Methods Mol Biol* **2311**: 9–23. https://doi.org/10.1007/978-1-0716-1437-2_2
- Li L, Shu F, Wang XQ, Wang F, Cai L, Zhao X, Lv HG (2021) Propofol alleviates intestinal ischemia/reperfusion injury in rats through p38 MAPK/NF-kappaB signaling pathway. *Eur Rev Med Pharmacol Sci* **25**: 1574–1581. https://doi.org/10.26355/eurrev_202102_24867
- Li X, Zhang S, Wa M, Liu Z, Hu S (2019) MicroRNA-101 protects against cardiac remodeling following myocardial infarction via down-regulation of runt-related transcription factor 1. *J Am Heart Assoc* **8**: e013112. <https://doi.org/10.1161/JAHA.119.013112>
- Li Y, Li H, Zhou L (2020) EZH2-mediated H3K27me3 inhibits ACE2 expression. *Biochem Biophys Res Commun* **526**: 947–952. <https://doi.org/10.1016/j.bbrc.2020.04.010>
- Liang H, Huang Q, Liao MJ, Xu F, Zhang T, He J, Zhang L, Liu HZ (2019) EZH2 plays a crucial role in ischemia/reperfusion-induced acute kidney injury by regulating p38 signaling. *Inflamm Res* **68**: 325–336. <https://doi.org/10.1007/s00011-019-01221-3>
- Liu D, Li Y, Luo G, Xiao X, Tao D, Wu X, Wang M, Huang C, Wang L, Zeng F, Jiang G (2017) LncRNA SPRY4-IT1 sponges miR-101-3p to promote proliferation and metastasis of bladder cancer cells through up-regulating EZH2. *Cancer Lett* **388**: 281–291. <https://doi.org/10.1016/j.canlet.2016.12.005>
- Liu LP, Zhang J, Pu B, Li WQ, Wang YS (2020a) Upregulation of JHDM1D-AS1 alleviates neuroinflammation and neuronal injury via targeting miR-101-3p-DUSP1 in spinal cord after brachial plexus injury. *Int Immunopharmacol* **89**: 106962. <https://doi.org/10.1016/j.intimp.2020.106962>
- Liu T, Cai J, Cai J, Wang Z, Cai L (2020b) EZH2-miRNA Positive feedback promotes tumor growth in ovarian cancer. *Front Oncol* **10**: 608393. <https://doi.org/10.3389/fonc.2020.608393>
- Liu X, Li C, Zhang R, Xiao W, Niu X, Ye X, Li Z, Guo Y, Tan J, Li Y (2018) The EZH2-H3K27me3-DNMT1 complex orchestrates epigenetic silencing of the wwl1 gene, a Hippo/YAP pathway upstream effector, in breast cancer epithelial cells. *Cell Signal* **51**: 243–256. <https://doi.org/10.1016/j.cellsig.2018.08.011>
- Liu XM, Chen QH, Hu Q, Liu Z, Wu Q, Liang SS, Zhang HG, Zhang Q, Zhang XK (2020c) Dexmedetomidine protects intestinal ischemia-reperfusion injury via inhibiting p38 MAPK cascades. *Exp Mol Pathol* **115**: 104444. <https://doi.org/10.1016/j.yexmp.2020.104444>
- Lv B, Jiang XM, Wang DW, Chen J, Han DF, Liu XL (2020) Protective effects and mechanisms of action of ulinastatin against cerebral ischemia-reperfusion injury. *Curr Pharm Des* **26**: 3332–3340. <https://doi.org/10.2174/138161282666200303114955>
- Merlo S, Spampinato SF, Sortino MA (2019) Early compensatory responses against neuronal injury: A new therapeutic window of opportunity for Alzheimer's Disease? *CNS Neurosci Ther* **25**: 5–13. <https://doi.org/10.1111/cns.13050>
- Moore HM, Gonzalez ME, Toy KA, Cimino-Mathews A, Argani P, Kleer CG (2013) EZH2 inhibition decreases p38 signaling and suppresses breast cancer motility and metastasis. *Breast Cancer Res Treat* **138**: 741–752. <https://doi.org/10.1007/s10549-013-2498-x>
- Nishioka C, Ikezoe T, Yang J, Yokoyama A (2015) Tetraspanin family member, CD82, regulates expression of EZH2 via inactivation of p38 MAPK signaling in leukemia cells. *PLoS One* **10**: e0125017. <https://doi.org/10.1371/journal.pone.0125017>
- Ozes AR, Pulliam N, Ertoşun MG, Yilmaz O, Tang J, Copuroglu E, Matei D, Ozes ON, Nephew KP (2018) Protein kinase A-mediated phosphorylation regulates STAT3 activation and oncogenic EZH2 activity. *Oncogene* **37**: 3589–3600. <https://doi.org/10.1038/s41388-018-0218-z>
- Peng T, Jiang Y, Farhan M, Lazarovici P, Chen L, Zheng W (2019) Anti-inflammatory effects of traditional chinese medicines on pre-clinical *in vivo* models of brain ischemia-reperfusion-injury: prospects for neuroprotective drug discovery and therapy. *Front Pharmacol* **10**: 204. <https://doi.org/10.3389/fphar.2019.00204>
- Qin Z, Zhu K, Xue J, Cao P, Xu L, Xu Z, Liang K, Zhu J, Jia R (2019) Zinc-induced protective effect for testicular ischemia-reperfusion injury by promoting antioxidation via microRNA-101-3p/Nrf2 pathway. *Aging (Albany NY)* **11**: 9295–9309. <https://doi.org/10.18632/aging.102348>
- Sekerdag E, Sölaroglu I, Gürsoy-Ozdemir Y (2018) Cell death mechanisms in stroke and novel molecular and cellular treatment options. *Curr Neuropharmacol* **16**: 1396–1415. <https://doi.org/10.2174/15701519X16666180302115544>
- Shan W, Ge H, Chen B, Huang L, Zhu S, Zhou Y (2021): Upregulation of miR-499a-5p decreases cerebral ischemia/reperfusion injury by targeting PDCCD4. *Cell Mol Neurobiol* (Online ahead of print). <https://doi.org/10.1007/s10571-021-01085-4>
- Shipley MM, Mangold CA, Szpara ML (2016): Differentiation of the SH-SY5Y human neuroblastoma cell line. *J Vis Exp* **108**: 53193. <https://doi.org/10.3791/53193>
- Smits M, Mir SE, Nilsson RJ, van der Stoop PM, Niers JM, Marquez VE, Cloos J, Breakefield XO, Krichevsky AM, Noske DP, Tannous BA, Wurdinger T (2011) Down-regulation of miR-101 in endothelial cells promotes blood vessel formation through reduced repression of EZH2. *PLoS One* **6**: e16282. <https://doi.org/10.1371/journal.pone.0016282>
- Song H, Du, C, Wang, X, Zhang, J, and Shen, Z (2019a) MicroRNA-101 inhibits autophagy to alleviate liver ischemia/reperfusion injury via regulating the mTOR signaling pathway. *Int J Mol Med* **43**: 1331-1342. <https://doi.org/10.3892/ijmm.2019.4077>
- Song H, Liu Y, Jin X, Liu Y, Yang Y, Li L, Wang X, Li G (2019b) Long non-coding RNA LINC01535 promotes cervical cancer progression via targeting the miR-214/EZH2 feedback loop. *J Cell Mol Med* **23**: 6098–6111. <https://doi.org/10.1111/jcmm.14476>
- Song N, Ma J, Meng XW, Liu H, Wang H, Song SY, Chen QC, Liu HY, Zhang J, Peng K, Ji FH (2020) Heat shock protein 70 protects the heart from ischemia/reperfusion injury through inhibition of p38 MAPK Signaling. *Oxid Med Cell Longev* **2020**: 3908641. <https://doi.org/10.1155/2020/3908641>
- Wang C, Yang YH, Zhou L, Ding XL, Meng YC, Han K (2020a) Curcumin alleviates OGD/R-induced PC12 cell damage via repressing CCL3 and inactivating TLR4/MyD88/MAPK/NF-kappaB to suppress inflammation and apoptosis. *J Pharm Pharmacol* **72**: 1176–1185. <https://doi.org/10.1111/jphp.13293>
- Wang H, Yu Q, Zhang ZL, Ma H, Li XQ (2020b) Involvement of the miR-137-3p/CAPN-2 interaction in ischemia-reperfusion-induced neuronal apoptosis through modulation of p35 cleavage and subsequent caspase-8 overactivation. *Oxid Med Cell Longev* **2020**: 2616871. <https://doi.org/10.1155/2020/2616871>
- Wang J, Wang GG (2020): No easy way out for EZH2: Its pleiotropic, noncanonical effects on gene regulation and cellular function. *Int J Mol Sci* **21**: 9501. <https://doi.org/10.3390/ijms21249501>
- Wang W, Qin X, Wang R, Xu J, Wu H, Khalid A, Jiang H, Liu D, Pan F (2020c) EZH2 is involved in vulnerability to neuroinflammation and depression-like behaviors induced by chronic stress in different aged mice. *J Affect Disord* **272**: 452–464. <https://doi.org/10.1016/j.jad.2020.03.154>
- Wang W, Tang L, Li Y, Wang Y (2015) Biochanin A protects against focal cerebral ischemia/reperfusion in rats via inhibition of p38-mediated inflammatory responses. *J Neurol Sci* **348**: 121–125. <https://doi.org/10.1016/j.jns.2014.11.018>
- Wu C, Ruan T, Liu W, Zhu X, Pan J, Lu W, Yan C, Tao K, Zhang W, Zhang C (2018) Effect and mechanism of curcumin on EZH2 – miR-101 regulatory feedback loop in multiple myeloma. *Curr Pharm Des* **24**: 564–575. <https://doi.org/10.2174/1381612823666170317164639>
- Wu J, Tang Q, Yang L, Chen Y, Zheng F, Hann SS (2017) Interplay of DNA methyltransferase 1 and EZH2 through inactivation of Stat3 contributes to beta-elemene-inhibited growth of nasopharyngeal carcinoma cells. *Sci Rep* **7**: 509. <https://doi.org/10.1038/s41598-017-00626-6>
- Xu L, Li T, Chen Q, Liu Z, Chen Y, Hu K, Zhang X (2021) The alpha2AR/Caveolin-1/p38MAPK/NF-kappaB axis explains dexmedetomidine protection against lung injury following intestinal ischemia-reperfusion. *J Cell Mol Med* **25**: 6361–6372. <https://doi.org/10.1111/jcmm.16614>
- Xue H, Xu Y, Wang S, Wu ZY, Li XY, Zhang YH, Niu JY, Gao QS, Zhao P (2019) Sevoflurane post-conditioning alleviates neonatal rat hypoxic-ischemic cerebral injury via Ezh2-regulated autophagy. *Drug Des Devel Ther* **13**: 1691–1706. <https://doi.org/10.2147/DDDT.S197325>
- Yang CC, Wei XP, Fu XM, Qian LT, Xie LJ, Liu HB, Li G, Li XG, Zeng XW (2021) Down-regulating microRNA-20a regulates CDH1 to protect against cerebral ischemia/reperfusion injury in rats. *Cell Cycle* **20**: 54–64. <https://doi.org/10.1080/15384101.2020.1856498>
- Yi Z, Shi Y, Zhao P, Xu Y, Pan P (2020) Overexpression of miR-217-5p protects against oxygen-glucose deprivation/reperfusion-induced neuronal injury via inhibition of PTEN. *Hum Cell* **33**: 1026–1035. <https://doi.org/10.1007/s13577-020-00396-w>
- Zhang H, Zhou J, Zhang M, Yi Y, He B (2019) Upregulation of miR-376c-3p alleviates oxygen-glucose deprivation-induced cell injury by

- targeting ING5. *Cell Mol Biol Lett* **24**: 67. <https://doi.org/10.1186/s11658-019-0189-2>
- Zhao JY, Wang XL, Yang YC, Zhang B, Wu YB (2020) Upregulated miR-101 inhibits acute kidney injury-chronic kidney disease transition by regulating epithelial-mesenchymal transition. *Hum Exp Toxicol* **39**: 1628–1638. <https://doi.org/10.1177/0960327120937334>
- Zhao Y, Ai Y (2019) Knockdown of lncRNA MALAT1 alleviates bupivacaine-induced neurotoxicity via the miR-101-3p/PDCD4 axis. *Life Sci* **232**: 116606. <https://doi.org/10.1016/j.lfs.2019.116606>
- Zhuang C, Wang P, Huang D, Xu L, Wang X, Wang L, Hu L (2016) A double-negative feedback loop between EZH2 and miR-26a regulates tumor cell growth in hepatocellular carcinoma. *Int J Oncol* **48**: 1195–1204. <https://doi.org/10.3892/ijo.2016.3336>